ELSEVIER

Journal of Molecular Structure 470 (1998) 49–60

Journal of
MOLECULAR
STRUCTURE

Hydrothermal synthesis and crystal structures of two novel vanadium oxides containing interlamellar transition metal complexes

Patricia J. Ollivier[a], Jeffrey R.D. DeBoard[b,c], Pamela J. Zapf[c,*,1], Jon Zubieta[c,*,1], Linda M. Meyer[b], Chwan-Chin Wang[b], Thomas E. Mallouk[a,*,2], Robert C. Haushalter[b,*,3]

[a]*Department of Chemistry, Pennsylvania State University, University Park, PA 16802, USA*
[b]*NEC Research Institute, 4 Independence Way, Princeton, NJ 08540, USA*
[c]*Department of Chemistry, Syracuse University, Syracuse, NY 13244, USA*

Received 31 October 1997; accepted 5 February 1998

Abstract

Two new vanadium oxide compounds, which contain interlamellar transition metal complexes bound to vanadium oxide sheets, were synthesized hydrothermally. The crystal structure of each reveals unusual coordination geometries and interlayer bonding. [Ni(2,2′-bipyridine)]$_2$[$V_{12}O_{32}$] (**1**) was prepared from the reaction of V_2O_5, NiO, H_2O and 2,2′-bipyridyl in the molar ratio 4:8:3312:0.5. The isomorphous compounds [M(2,2′-bipy)]$_2$[$V_{12}O_{32}$] (where M is Co (**1a**) and Cu (**1b**)) were prepared in a similar fashion. The Ni coordination compound **1** crystallizes as amber needles, and the structure was solved in the space group *C*2/*m* (#12) with unit cell parameters $\underline{a}=24.344(3)$ Å, $\underline{b}=6.897(3)$ Å, $\underline{c}=12.028(2)$ Å, $\beta=93.60(2)°$ ($R(Rw)=0.039(0.038)$). This compound is composed of vanadium(V) oxide layers with nickel atoms coordinated within a single layer via four Ni–O–V linkages. Bidentate bipyridine (bpy) ligands complete the coordination sphere of the nickel atoms and interdigitate via $\pi-\pi$ stacking with bpy ligands from the adjacent layer. Cu(en)$_2$[V_6O_{14}] (**2**) crystallizes as black plates in the space group $P2_1/n$ (#14) with unit cell parameters $\underline{a}=8.934(2)$ Å, $\underline{b}=6.558(1)$ Å, $\underline{c}=15.694(2)$ Å, $\beta=99.93(2)°$ ($R(Rw)=0.039(0.035)$), from the reaction of $CuCl_2\cdot 2H_2O$, V_2O_5, H_2O and ethylenediamine in the ratio 1:1:447:4. This structure consists of mixed-valent vanadium(IV,V) oxide sheets forming weak O–Cu bonds to intercalated copper bis(ethylenediamine) complexes.

Keywords: Vanadium oxide; Nickel (cobalt,copper) bipyridine complex; Lamellar; Crystal structure; Hydrogen bonding; Hydrothermal; Copper ethylenediamine complex

1. Introduction

Hydrothermal synthetic techniques can be used to form novel structures and compounds from relatively insoluble and unreactive precursors. Reactants are combined in varying molar ratios, fill volumes, pressures and temperatures, and produce metastable compounds that are often not accessible by higher temperature syntheses. In hydrothermal zeolite

Dedicated to Professor Abraham Clearfield on the occasion of his 70th birthday.

* Corresponding authors.
[1] Tel.: +1-315-443-2547; Fax: +1-315-443-4070; E-mail: jazubiet@mailbox.syr.edu
[2] Tel.: +1-814-863-9637; Fax: +1-814-863-8403; E-mail: tom@chem.psu.edu
[3] Current address: Symyx Technologies, 3100 Central Expressway, Santa Clara, CA 95051, USA. Tel.: +1-408-328-3150; Fax: +1-408-732-3949; E-mail: bobh@symyx.com

0022-2860/98/$ - see front matter
PII S0022-2860(98)00469-4

synthesis, the size and shape of pores and cages are directed by the organic template around which crystallization takes place [1,2]. Similar templating effects are operative in the hydrothermal synthesis of lamellar compounds. While reaction mechanisms in these hydrothermal systems are still not understood in detail, systematic variations of pH, pressure, temperature and reactants can be studied readily. Judicious choice of precursors can help 'direct' product formation, often yielding a single product phase [3].

Recently, there has been much interest in the preparation of layered inorganic/organic hybrid materials, because of the possibility of tailoring structures and properties. The controlled siting of organic groups and transition metal complexes within extended metal oxide frameworks can lead to interesting material properties associated with interactions between metal centers and the availability of several oxidation states. For example, Clearfield and co-workers have shown that a number of photochemically [4,5] and magnetically [6] interesting solids can be prepared through intercalation or grafting of structurally well-defined metal complexes. In related work, the magnetic interactions in lamellar vanadium phosphonates have been tuned rationally by varying the electron-donating power of pendent organic groups [7–9]. Low-dimensional solids are also amenable to post-synthesis modifications, which impart an extra degree of structural control. For example, layered transition metal oxides and phosphates can be intercalated and exfoliated, and then re-assembled in different sequences [10]. This capability allows one to stack photoredox molecules in the appropriate order for multistep light- induced electron and energy transfer reactions [11,12].

Some mixed transition metal oxide–coordination solids have already been prepared by hydrothermal synthesis. These include coordination compounds with pseudo-three-dimensional structures [13] in which the ligands act as bridges between layers, and materials consisting of metal oxo clusters or one-dimensional chains within coordination polymer scaffolding [14,15]. In this paper, we explore hydrothermal synthesis as a means of preparing lamellar vanadium oxides in which transition metal complexes are bound to the oxide sheets. Substitution-labile metal ions, Co(II), Cu(II) and Ni(II), and simple bidentate ligands 2,2′-bipyridine (bpy) and ethylenediamine (en) were chosen for this initial study. The structures of the resulting hybrid vanadium oxide–transition metal complex solids illustrate that both the metal and the ligand have important structure-directing effects on the vanadium oxide framework, which adapts to maximize covalent and non-covalent interactions with and between the guest molecules.

Table 1
Crystallographic data for **1**, **1a**, **1b**, and **2**

Parameter	$V_{12}O_{32}Ni_2N_4C_{20}H_{16}$	$V_{12}O_{32}Co_2N_4C_{20}H_{12}$	$V_{12}O_{32}Cu_2N_4C_{20}H_{12}$	$V_6O_{14}CuN_4C_4H_{16}$
a (Å)	24.344(3)	24.495(2)	24.2377(6)	8.934(2)
b (Å)	6.897(3)	6.9399(5)	7.0235(2)	6.558(1)
c (Å)	12.028(2)	12.0554(8)	11.9725(1)	15.694(2)
β	93.60(2)	93.568(2)	93.363(1)	99.93(2)
V (Å^3)	2015.4(9)	2045.4(2)	2034.61(8)	905.8(3)
Z	2	2	2	2
Formula weight	1553.05	1553.50	1562.72	713.38
Space group	$C2/m$ #12	$C2/m$ #12	$C2/m$ #12	$P2_1/c$ #14
T (°C)	20 ± 1	− 123 ± 2	− 1213 ± 2	20 ± 1
λ (Å)	0.71073	0.71073	0.71073	0.71073
Range of data collected	$h\ k\ \pm l$	$\pm h\ \pm k\ \pm l$	$\pm h\ \pm k\ \pm l$	$h\ k\ \pm l$
Maximum 2θ (deg)	60.1	57.6	57.6	50.1
Reflections collected	3258	6480	6430	1714
Number of unique data	3190	2577	2543	1597
Dcalc (g cm^{-3})	2.56	2.522	2.551	2.62
μ (cm^{-1})	36.6	34.98	37.47	41.87
R	0.038	0.079	0.067	0.035
Rw	0.039	0.138	0.115	0.039

Table 2
Atomic coordinates for $[Ni(bpy)]_2[V_{12}O_{32}]$ (**1**)

Atom	*x*	*y*	*z*
Ni(1)	0.39750(3)	0.0000	0.42247(6)
V(1)	0.44370(4)	0.5000	– 0.29282(7)
V(2)	0.43477(3)	0.24046(9)	– 0.08995(5)
V(3)	0.42822(4)	0.5000	0.13280(7)
V(4)	0.44240(4)	0.5000	0.42085(7)
V(5)	0.52541(4)	0.0000	0.31007(7)
O(1)	0.4735(1)	0.5000	– 0.4239(3)
O(2)	0.3802(2)	0.5000	– 0.3285(3)
O(3)	0.3701(1)	0.2210(4)	– 0.1029(2)
O(4)	0.4622(2)	0.0000	– 0.0930(3)
O(5)	0.4492(1)	0.2943(4)	0.0562(2)
O(6)	0.3634(2)	0.5000	0.1347(4)
O(7)	0.4487(1)	0.5000	– 0.1305(3)
O(8)	0.45182(10)	0.2321(4)	– 0.2540(2)
O(9)	0.4488(1)	0.0000	– 0.4373(3)
O(10)	0.5420(1)	0.5000	– 0.2665(3)
O(11)	0.40374(10)	0.3084(4)	0.4260(2)
O(12)	0.4584(1)	0.0000	0.3163(3)
N(1)	0.6723(2)	0.0000	– 0.5108(4)
N(2)	0.6600(2)	0.0000	– 0.2945(4)
C(1)	0.6744(3)	0.0000	– 0.6215(5)
C(2)	0.7237(3)	0.0000	– 0.6727(6)
C(3)	0.7716(3)	0.0000	– 0.6076(5)
C(4)	0.7702(3)	0.0000	– 0.4936(5)
C(5)	0.7192(2)	0.0000	– 0.4456(4)
C(6)	0.7131(2)	0.0000	– 0.3241(5)
C(7)	0.7568(3)	0.0000	– 0.2454(6)
C(8)	0.7466(3)	0.0000	– 0.1330(6)
C(9)	0.6931(3)	0.0000	– 0.1037(6)
C(10)	0.6514(3)	0.0000	– 0.1853(5)
H(1)	0.638(3)	0.0000	– 0.672(6)
H(2)	0.726(3)	0.0000	– 0.758(6)
H(3)	0.810(3)	0.0000	– 0.635(5)
H(4)	0.798(2)	0.0000	– 0.434(5)
H(5)	0.794(2)	0.0000	– 0.274(5)
H(6)	0.776(2)	0.0000	– 0.077(5)
H(7)	0.686(4)	0.0000	– 0.023(3)
H(8)	0.620(2)	0.0000	– 0.162(5)

Table 3
Atomic positional parameters for $[Co(bipy)]_2[V_{12}O_{32}]$ (**1a**)

Atom	*x*	*y*	*z*
Co(1)	0.3986(1)	0.0000	0.4232(1)
V(1)	0.5562(1)	– 0.5000	0.2919(1)
V(2)	0.5648(1)	– 0.2404(2)	0.893(1)
V(3)	0.4289(1)	– 0.5000	0.1327(2)
V(4)	0.4431(1)	– 0.5000	0.4210(1)
V(5)	0.5254(1)	0.0000	0.3064(2)
O(1)	0.5261(3)	– 0.5000	0.4231(6)
O(2)	0.6197(3)	– 0.5000	0.3276(6)
O(3)	0.6295(2)	– 0.2229(8)	0.1011(4)
O(4)	0.5380(3)	0.0000	0.935(8)
O(5)	0.4500(2)	– 7049(8)	0.568(4)
O(6)	0.3642(4)	– 0.5000	0.1369(7)
O(7)	0.5514(3)	– 0.5000	0.1294(5)
O(8)	0.5482(2)	– 0.2328(8)	0.2535(4)
O(9)	0.4486(3)	0.0000	0.5654(6)
O(10)	0.4582(3)	– 0.5000	0.2662(6)
O(11)	0.4043(2)	0.3066(8)	0.4262(4)
O(12)	0.4584(3)	0.0000	0.3122(6)
N(1)	0.3381(4)	0.0000	0.2919(7)
N(2)	0.3269(4)	0.0000	0.5100(7)
C(1)	0.3472(5)	0.0000	0.1835(9)
C(3)	0.2516(6)	0.0000	0.1327(10)
C(4)	0.2419(5)	0.0000	0.2443(10)
C(5)	0.2864(5)	0.0000	0.3242(9)
C(6)	0.2795(4)	0.0000	0.4454(9)
C(7)	0.2300(5)	0.0000	0.4927(11)
C(8)	0.2262(5)	0.0000	0.6074(9)
C(9)	0.2747(5)	0.0000	0.6727(11)
C(10)	0.3233(5)	0.0000	0.6227(10)

2. Experimental

2.1. Syntheses

All reactions were carried out in polytetrafluoroethylene-lined stainless-steel containers under autogeneous pressure unless otherwise stated. The vessels were each of volume 23 ml and were filled approximately to 40% capacity.

2.1.1. $[Ni(bpy)]_2[V_{12}O_{32}]$ (**1**)

A mixture of 0.122 g of V_2O_5, 0.100 g of NiO, 10.0 ml of H_2O and 0.013 g of 2,2′-bipyridine (mole ratio 4:8:3312:0.5) was stirred for a few seconds at room temperature with a glass stirring rod before heating to 170°C for 24 h, then to 200°C for a further 24 h, yielding a green suspension of amber crystals of **1** and excess nickel oxide. While several attempts were made to improve the phase purity of the product by changing reactant ratios, reaction times and temperatures, none were particularly successful. Crystals of **1** were separated physically from the mixture for X-ray diffraction analysis. The products were rinsed with water until no more solid green NiO could be washed away. This left a mixture of nickel oxide and **1**, as identified by X-ray powder diffraction analysis. (The yield of amber crystals was 5–10%.)

Table 4
Atomic positional parameters for $[Cu(bipy)]_2[V_{12}O_{32}]$ (**1b**)

Atom	*x*	*y*	*z*
Cu(1)	0.3956(1)	0.0000	0.4255(1)
V(1)	0.5553(1)	− 0.5000	0.2915(1)
V(2)	0.5639(1)	− 0.2409(2)	0.908(1)
V(3)	0.4283(1)	− 0.5000	0.1305(1)
V(4)	0.4416(1)	− 0.5000	0.4222(1)
V(5)	0.5249(1)	0.0000	0.3091(1)
O(1)	0.5262(3)	− 0.5000	0.4239(5)
O(2)	0.6196(3)	− 0.5000	0.3242(5)
O(3)	0.6293(2)	− 0.2232(7)	0.1038(4)
O(4)	0.5382(3)	0.0000	0.958(9)
O(5)	0.4505(2)	− 0.7063(7)	0.559(3)
O(6)	0.3627(3)	− 0.5000	0.1301(6)
O(7)	0.5500(3)	− 0.5000	0.1290(5)
O(8)	0.5456(2)	− 0.2330(7)	0.2534(3)
O(9)	0.4455(3)	0.0000	0.5644(5)
O(10)	0.4567(3)	− 0.5000	0.2647(5)
O(11)	0.4015(2)	0.3162(7)	0.4285(4)
O(12)	0.4576(2)	0.0000	0.3235(5)
N(1)	0.3400(3)	0.0000	0.2973(6)
N(2)	0.3272(3)	0.0000	0.5119(6)
C(1)	0.3501(4)	0.0000	0.1885(8)
C(2)	0.3081(5)	0.0000	0.1043(8)
C(3)	0.2543(4)	0.0000	0.1319(9)
C(4)	0.2433(4)	0.0000	0.2445(9)
C(5)	0.2864(4)	0.0000	0.3254(8)
C(6)	0.2792(4)	0.0000	0.4475(8)
C(7)	0.2284(4)	0.0000	0.4946(8)
C(8)	0.2261(4)	0.0000	0.6097(9)
C(9)	0.2751(4)	0.0000	0.6756(9)
C(10)	0.3245(4)	0.0000	0.6234(8)

2.1.2. $[Co(bpy)]_2[V_{12}O_{32}]$ (**1a**)

A mixture of 0.102 g of V_2O_5, 0.263 g of $CoCl_2 \cdot 6H_2O$, 5.078 g of H_2O and 0.088 g of 2,2′-bipyridine in the mole ratio 1:1.98:505:1 was heated at 200°C for 160 h in a borosilicate glass tube (approximately 40% fill volume). Red crystals of **1a** were separated from the amorphous red powder. (The yield of the red crystals was 5–10%.)

2.1.3. $[Cu(bpy)]_2[V_{12}O_{32}]$ (**1b**)

A mixture of 0.027 g of V_2O_5, 0.045 g of $CuCl_2 \cdot 2H_2O$, 5.092 g of H_2O and 0.044 g of 2,2′-bipyridine in the mole ratio 1:1.8:1913:1.9 was heated at 200°C for 128 h in a borosilicate glass tube (approximately 40% fill volume). Yellow crystals of **1b** were mechanically separated from an amorphous green solid. (The yield was 10–20%.)

2.1.4. $Cu(en)_2[V_6O_{14}]$ (**2**)

A mixture of 0.170 g of $CuCl_2 \cdot 2H_2O$, 0.181 g of ground V_2O_5, 8.0 ml of H_2O and 0.28 ml of ethylenediamine (mole ratio 1:1:447:4) was stirred for a few seconds at room temperature and then heated at 170°C for 65 h. The resulting solution was dark blue with black plates. The product was washed with water and black plates of **2** were isolated as the only solid phase in approximately 90% yield based on vanadium.

2.2. Crystallography

Data were collected at 20°C using a Rigaku AFC7R instrument equipped with a graphite monochromated Mo Kα radiation source ($\lambda = 0.71073$ Å) and an 18 kW rotating anode generator. Single crystal structures were solved using teXsan crystallographic software [16].

Crystallographic data for all compounds are contained in Table 1. Their structures were solved using direct methods [17] with corrections made for Lorentz and polarization effects as well as an empirical correction for absorption using DIFABS [18]. For compound **1**, all vanadium and nickel atoms were refined anisotropically, and light atoms (C, N, O, H) were refined isotropically. In the cases of **1a**, **1b** and **2**, all the non-hydrogen atoms were refined anisotropically. Hydrogen atoms were included in the structure solutions of **1a**, **1b** and **2** but not refined.

2.3. Infrared spectra

Spectra of **1** and of 2,2′-bipyridine in KBr pellets were recorded on a Nicolet 730 FT-IR spectrometer with an MCT-A detector, operating at 2 cm^{-1} resolution.

3. Results and discussion

The compounds reported here consist of vanadium oxide sheets, with metal ligand complexes M(2,2′-bpy) (where M is Ni, Cu, Co) and $Cu(en)_2$ occupying the interlamellar regions. In both cases, the metal coordination sphere is composed of both molecular ligands (bpy or en) and oxygen atoms from the vanadium oxide sheets.

The isomorphous compounds **1**, **1a**, and **1b**,

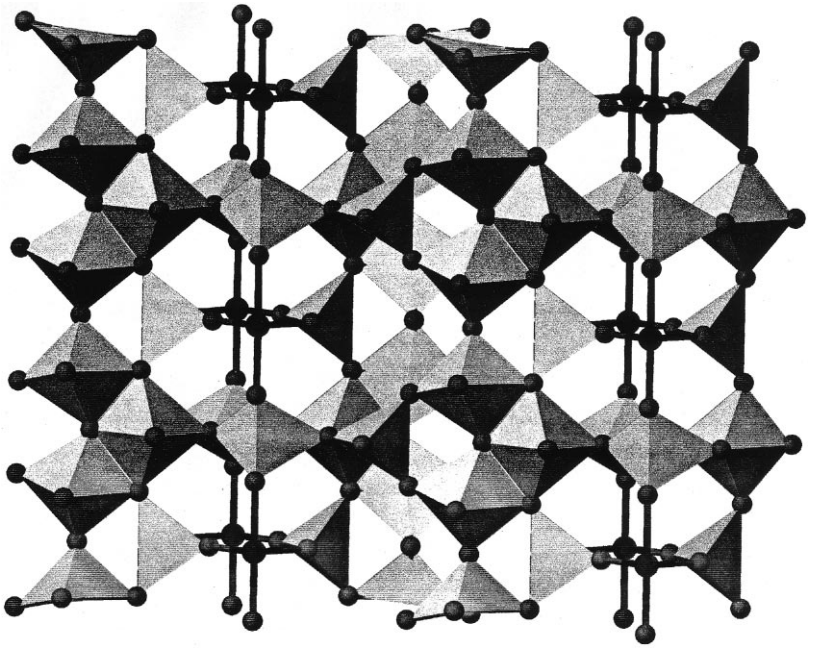

Fig. 1. Polyhedral view of a layer in the structure of **1**, showing bonding between vanadium, oxygen and nickel atoms.

$[M(bpy)]_2[V_{12}O_{32}]$ (where M is Ni (**1**), Cu (**1a**), Co (**1b**)), contain vanadium(V) oxide double sheets in which divalent metal atoms occupy rectangular 'holes'. Atomic positions are given in Tables 2, 3, and 4. Fig. 1 shows a polyhedral view of the sheets in compound **1**, approximately down the crystallographic *a* axis. The Ni atoms, shown in black, are ligated to four oxygen atoms from VO_4 and VO_5 polyhedra. Ribbons of edge- and corner sharing VO_5 square pyramids run along the *c* axis, with apical oxygen atoms pointing away from the center of the bilayer and towards the interlamellar region. Fig. 2 shows an ORTEP plot of the vanadium coordination environments. The coordination of the nickel atoms is completed by two nitrogen atoms from a bpy unit, as shown in Fig. 3. The nickel–oxygen bond distances

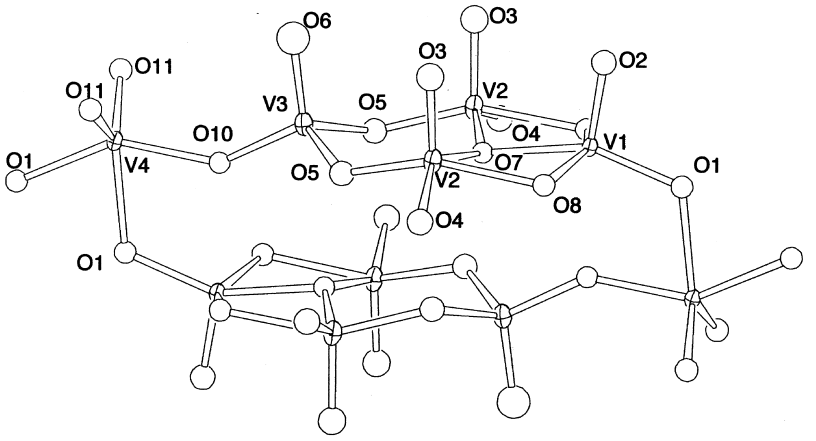

Fig. 2. ORTEP diagram of the vanadium oxide double sheets in compound **1**, showing coordination environments and the atom labeling scheme.

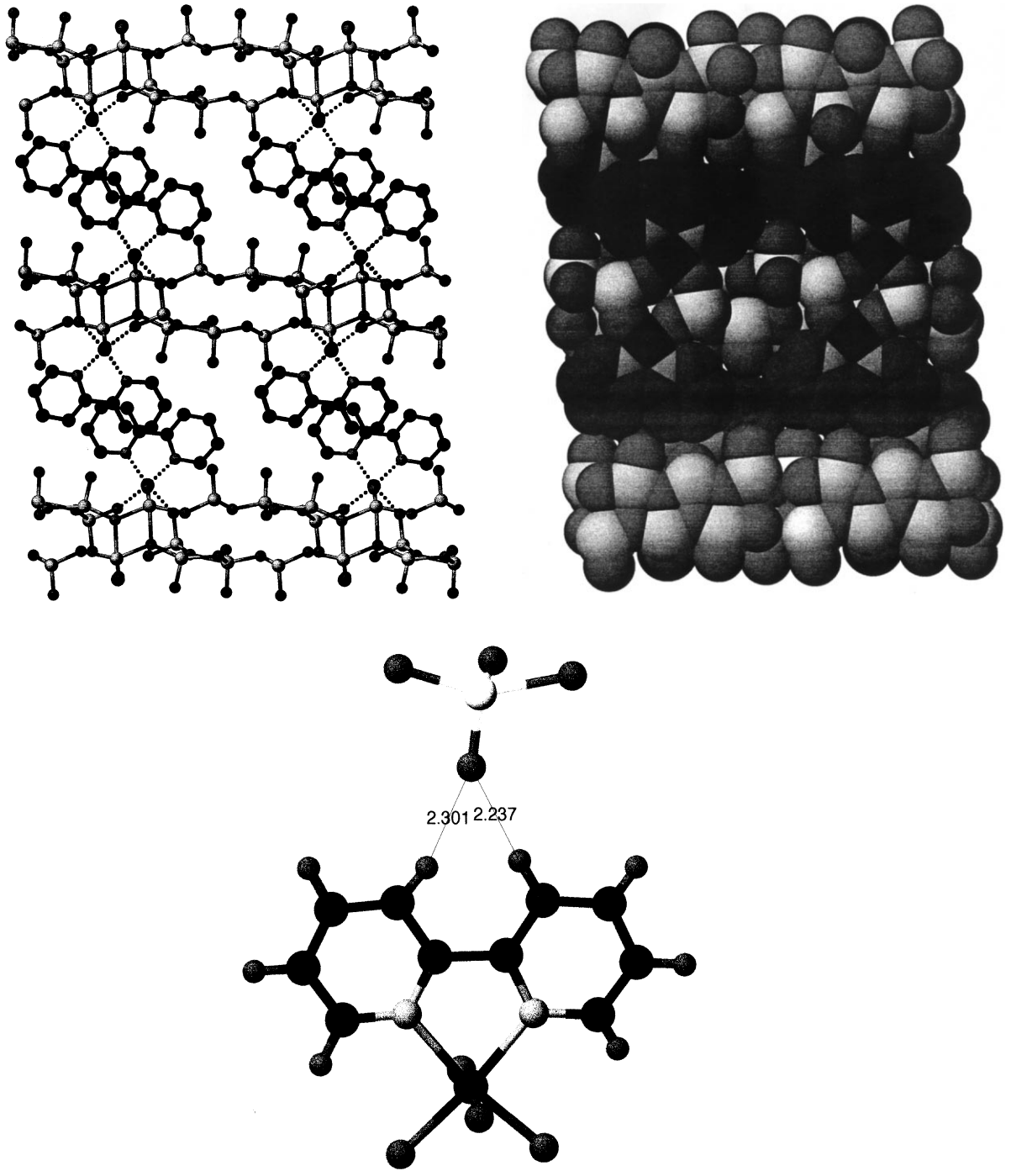

Fig. 3. (a) View of structure of **1** along the crystallographic *b*-axis, showing the Ni coordination environment and staggered stacks of bpy ligands. Hydrogen atoms are omitted for clarity. (b) Space-filling model of the same projection, including hydrogen atoms, and showing the packing of bpy ligands with apical oxygen atoms of VO_5 polyhedra in the adjacent sheets. (c) Short C–H…O non-bonded contacts in the structure.

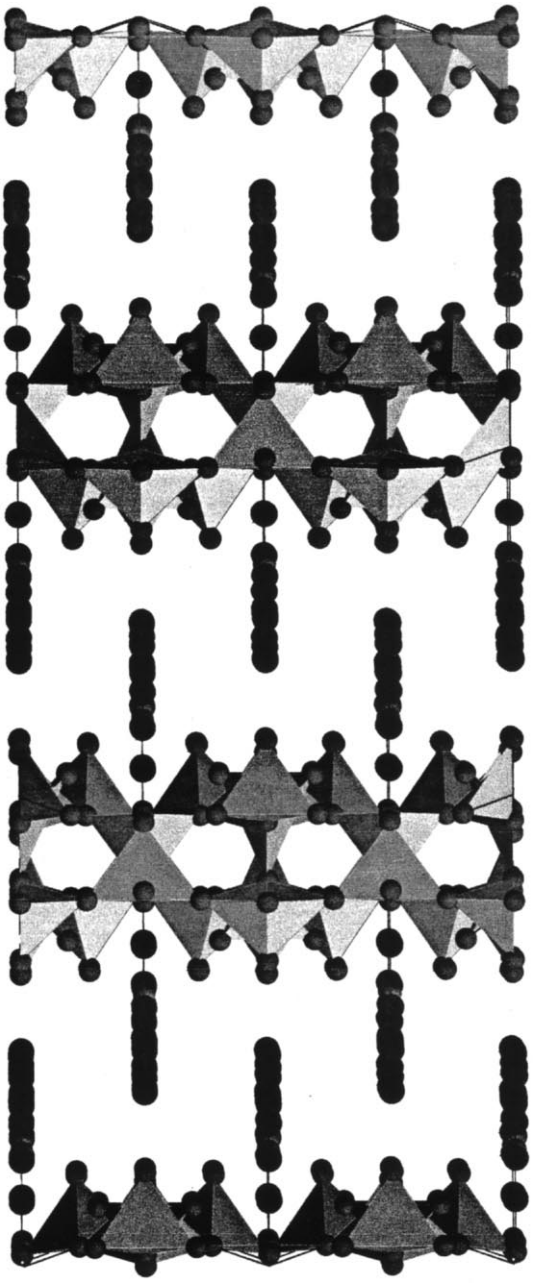

Fig. 4. View of the structure of **1** along the *c*-axis, showing alternating bpy ligands bound to each layer. Hydrogen atoms are omitted for clarity.

range from 2.02 to 2.13 Å and the nickel–nitrogen bonds are 2.02 and 2.06 Å long; hence the nickel coordination structure can be described as a slightly distorted octahedron.

The bipyridine ligands in **1**, **1a**, and **1b** are constrained by symmetry to be planar and lie parallel to each other, and their spacing along the *b*-axis is 3.45 Å, about 0.1 Å greater than the interplanar spacing in graphite. There is clearly a π-stacking interaction between the ligands, yet they pack between layers in a staggered fashion (see Figs. 3 and 4). A space-filling model of **1** shows that this staggered packing allows for a close fit between the bipyridyl hydrogen atoms and the apical oxygen atoms of the VO_5 ribbons in the next layer, as well as between bpy ligands in the same layer. The packing arrangement therefore maximizes van der Waals contacts of the organic groups along all three cystallographic axes.

The minor structural modifications exhibited by the isomorphous series **1**, **1a**, and **1b** reflect the anticipated trends in covalent radii and geometric preferences. Thus, as shown in Table 6 and Fig. 5, the metrical parameters associated with $[Co(bipy)]_2[V_{12}O_{32}]$ and $[Ni(bpy)]_2[V_{12}O_{32}]$ are nearly identical with the exception of the shorter bond distances associated with Ni(II) in comparison to Co(II). This observation is consistent with the contraction of the covalent radii of d-block cations as a function of atomic number and the Irving–Williams stability series. The more significant changes associated with $[Cu(bipy)]_2[V_{12}O_{32}]$ (**1b**) in comparison to **1** and **1a** reflect both the contraction of the covalent radius of Cu(II) in comparison to Co(II) and Ni(II) and the preference of Cu(II) for square planar or axially distorted six-coordinate geometries, a reflection of the static Jahn–Teller effect. Consequently, the in-plane Cu–O and Cu–N distances are significantly shorter than those observed for the Co(II) and Ni(II) analogues, while the axial Cu–O distances are elongated. The metrical parameters associated with the vanadium oxide networks of the three compounds are effectively identical.

Interestingly, in compound **1** there are short (2.2–2.3 Å) H…O non-bonded contacts between the VO_5 apical oxygen atoms and the hydrogen atoms in the 3,3′ positions of the bpy rings. The lengths of these C–H…O ‘hydrogen bonds’ are comparable to the

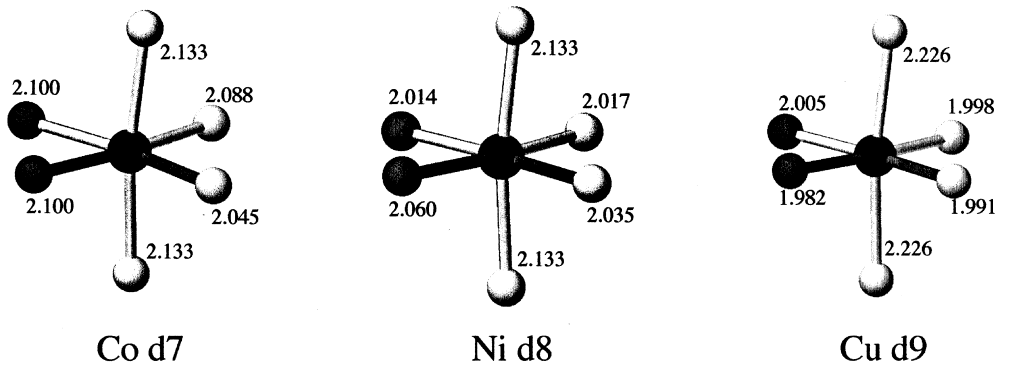

Fig. 5. View of coordination around the metal atoms in **1**, **1a**, and **1b** showing distorted octahedra and bond distances.

shortest such contacts found in terminal metal carbonyl complexes [19–21]. The C–H…O bond angle corresponding to the shortest H…O contact in **1** (2.237 Å) is 177°, consistent with hydrogen bonding, but the C–H bond length is 0.989 Å, which is intermediate between the shortest (0.981 Å) and the longest (1.042 Å) C–H bonds in the ligand. These bond lengths should be interpreted cautiously, since they are derived from X-ray data rather than from neutron diffraction data. Recently, the issue of whether short C–H…O contacts should be considered true hydrogen bonds has been debated [22]. An important question in the present case, and in others [19–21] is whether the H…O contact represents a net attractive or repulsive interaction. In an attempt to resolve this question, infrared spectra of **1** and the 2,2′-bipyridine ligand itself were recorded, and are shown in Fig. 6. The spectra are complex, and specific C–H stretching modes have not been assigned; however, many of the bands in the two spectra are clearly correlated. The broken lines in Fig. 6 show correlations between the C–H stretching modes in 2,2′-bipyridine and in **1**. The only uncorrelated bands appear at 3063 cm^{-1} in the bipyridine spectrum and

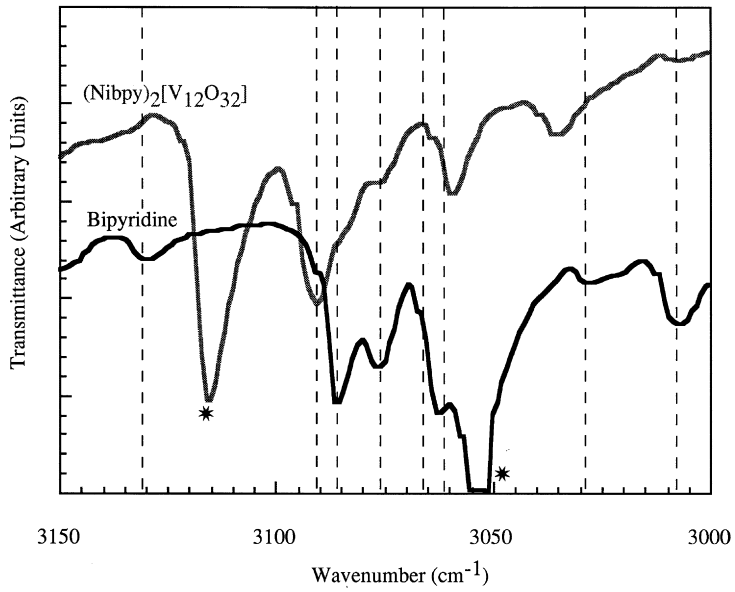

Fig. 6. C–H stretching region in the infrared spectra of **1** and 2,2′-bipyridine. The broken lines mark absorption bands in the spectrum of **1** that are correlated to bands in the 2,2′-bipyridine spectrum. The one strong, uncorrelated band in each spectrum is marked by an asterisk.

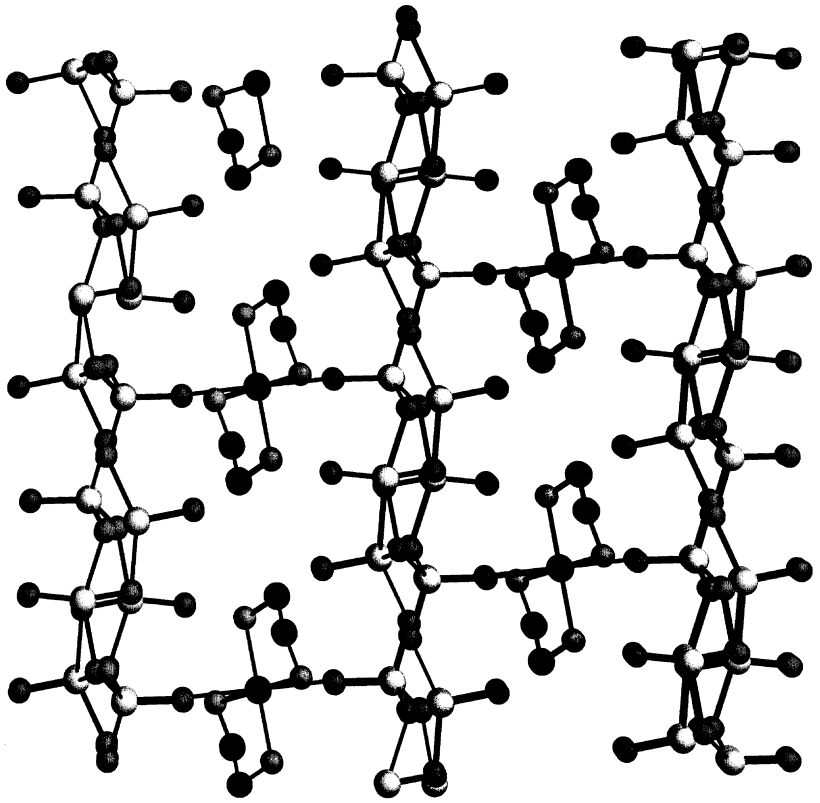

Fig. 7. Interlamellar view of the structure of **2**, showing $Cu(en)_2$ between the layers. The stacking axis direction is [101].

at 3114 cm^{-1} in **1**. If the latter arises from the C–H…O group, then it follows that the C–H bond is actually 'compressed' by a repulsive H…O interaction in **1**, shifting the vibration to higher frequency. Until deuterium labeling experiments are done to confirm the assignment of these C–H stretching bands, however, this conclusion should be drawn very tentatively.

Compound **2** contains vanadium oxide single-layer sheets with $Cu(en)_2$ complexes between (see Fig. 7). Atom positions are listed in Table 5, and bond lengths in Table 7. The presence of mixed valent (IV,V) vanadium is consistent with the black color of the crystals. Formal valences from valence sum calculations [23] are V(1) = 3.99, V(2) = 4.04, V(3) = 4.74. V(1) and V(2) are both five-coordinate while the more highly charged V(3) is four-coordinate. The vanadium oxide layers of **2** are made up of VO_4 tetrahedra and distorted VO_5 square pyramids. The square pyramids share edges, forming zig-zag ribbons which are linked together by corner-sharing tetrahedra. Apical oxygen atoms in the ribbons point into the interlamellar region, and the VO_5 units in the chains are arranged in pairs, with two apical oxygen atoms pointing up and the next two pointing down. The VO_4 tetrahedra each contain one apical oxygen atom, and share corners with three square pyramids from two zig-zag chains. A polyhedral view of the layer, viewed approximately down the stacking axis, or the [101] direction of the crystal, is shown in Fig. 8. Fig. 9 is an ORTEP diagram showing the details of the vanadium coordination geometry in the layers.

The mixed-valent vanadium oxide sheets of **2** flank the $[Cu(en)_2]^{2+}$ complex. Each copper atom in the structure is coordinated to two bidentate en ligands in a roughly square-planar arrangement. The coordination of the Jahn–Teller Cu(II) ion is actually an elongated octahedron, with four shorter bonds (2.003, 2.020 Å) to nitrogen atoms, and two longer contacts (2.523 Å) to apical oxygen atoms of the

Table 5
Atomic coordinates for $Cu(en)_2[V_6O_{14}]$, **2**

Atom	x	y	z
Cu(1)	0.0000	0.000	0.000
V(1)	–0.1879(2)	–0.4791(3)	0.2342(1)
V(2)	–0.0390(2)	–0.7605(3)	0.3607(1)
V(3)	–0.1310(2)	–0.2584(3)	0.4269(1)
O(1)	–0.053(1)	–0.388(1)	0.1889(5)
O(2)	–0.3292(8)	–0.269(1)	0.2523(4)
O(3)	–0.3612(9)	–0.527(1)	0.1346(5)
O(4)	–0.0108(9)	–0.753(1)	0.4882(4)
O(5)	0.1294(9)	–0.779(1)	0.3415(4)
O(6)	–0.1040(9)	–0.478(1)	0.3606(5)
O(7)	–0.2867(9)	–0.283(1)	0.4633(5)
N(1)	0.084(1)	0.012(2)	0.1279(6)
N(2)	–0.134(1)	–0.242(2)	0.0071(6)
C(1)	0.205(2)	0.168(2)	0.1428(8)
C(2)	–0.164(2)	–0.338(2)	–0.0784(9)
H(1)	0.0053	0.0480	0.1598
H(2)	0.1234	–0.1186	0.1483
H(3)	–0.0897	–0.3355	0.0507
H(4)	–0.2311	–0.1980	0.0231
H(5)	0.2176	0.2185	0.2004
H(6)	0.3003	0.1064	0.1349
H(7)	–0.0773	–0.4112	–0.0884
H(8)	–0.2475	–0.4366	–0.0817

sheets. The $[Cu(en)_2]^{2+}$ units are staggered from layer to layer as seen in Fig. 5, making relatively weak 2.164 Å N–H…O hydrogen bonds to terminal oxygen atoms and weaker 2.310 Å contacts to bridging oxygen atoms in the sheets. There are no short C–H…O contacts in this structure, consistent with the availability of better N–H hydrogen bond donors. (See Table 7.)

An interesting aspect of these structures is the combination of four- and five-coordinate vanadium. This combination makes for unusual shapes such as the group of three edge-sharing VO_5 units and one corner-sharing VO_4 tetrahedron in structure **2**. This repeat unit gives the layers in **2** a slight ripple. In both structures, apical oxygen atoms of the VO_4 and VO_5 polyhedra are electron-rich and sterically accessible, and make close contacts to the guest metal ions, as well as to N–H and C–H groups. The broad variety of possible structures that can be made from VO_4 and VO_5 building blocks allows the oxide sheets to conform to the steric requirements of the encapsulated metal–ligand complexes. This is particularly apparent in the structure of compound **1**, in which the vanadium oxide sheets adapt to give a crystallographic repeat along the *b*-axis that is essentially a perfect match for the bipyridyl interplanar spacing.

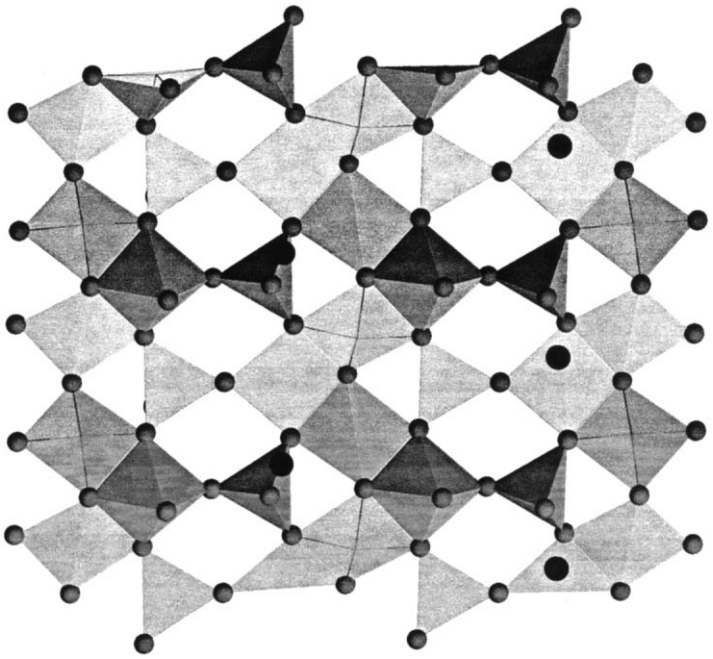

Fig. 8. Polyhedral view of the vanadium oxide layer in the structure of compound **2**.

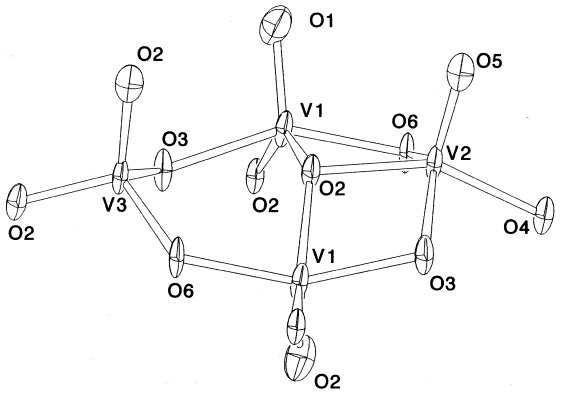

Fig. 9. ORTEP diagram showing the vanadium coordination environments in **2**.

Table 6
Comparison of selected bond lengths (Å) for $[Ni(bpy)]_2[V_{12}\}O_{32}]$ (**1**), $[Co(bpy)]$, $[V_{12}O_{32}]$ (**1a**) and $[Cu(bpy)]_2[V_{12}O_{32}]$ (**1b**)

Atom	Atom	Distance		
		M=Ni	M=Co	M=Cu
M	O(9)	2.035(5)	2.044(7)	1.997(6)
M	O(11)	2.132(3)	2.132(5)	2.005(7)
M	O(11)	2.132(3)	2.132(5)	2.226(5)
M	O(12)	2.017(4)	2.045(8)	2.226(5)
M	N(1)	2.060(6)	2.099(9)	2.005(7)
M	N(2)	2.016(6)	2.098(9)	1.983(8)
V(1)	O(1)	1.777(4)	1.786(7)	1.772(6)
V(1)	O(2)	1.579(5)	1.586(8)	1.585(6)
V(1)	O(7)	1.949(5)	1.956(7)	1.943(6)
V(1)	O(8)	1.913(3)	1.919(5)	1.940(5)
V(1)	O(8)	1.913(3)	1.919(5)	1.940(5)
V(2)	O(3)	1.579(3)	1.587(5)	1.589(4)
V(2)	O(4)	1.789(2)	1.795(3)	1.805(3)
V(2)	O(5)	1.810(3)	1.816(5)	1.808(4)
V(2)	O(7)	1.892(2)	1.899(3)	1.911(2)
V(2)	O(8)	2.043(3)	2.045(5)	2.023(4)
V(3)	O(5)	1.783(3)	1.785(6)	1.801(5)
V(3)	O(5)	1.783(3)	1.785(6)	1.801(5)
V(3)	O(6)	1.581(6)	1.589(9)	1.587(7)
V(3)	O(10)	1.722(5)	1.721(8)	1.711(6)
V(4)	O(1)	1.970(4)	1.981(8)	1.958(6)
V(4)	O(1)	2.045(4)	2.032(8)	2.051(7)
V(4)	O(10)	1.918(4)	1.928(8)	1.942(6)
V(4)	O(11)	1.626(3)	1.649(8)	1.620(8)
V(4)	O(11)	1.626(3)	1.649(8)	1.620(8)
V(5)	O(8)	1.836(3)	1.837(5)	1.848(8)
V(5)	O(8)	1.836(3)	1.837(5)	1.848(8)
V(5)	O(9)	1.617(5)	1.637(7)	1.639(7)
V(5)	O(12)	1.637(4)	1.646(8)	1.651(6)

Table 7
Selected bond lengths for $Cu(en)_2[V_6O_{14}]$ (**2**)

Atom	Atom	Distance
Cu(1)	N(1)	2.027(6)
Cu(1)	N(1)	2.027(6)
Cu(1)	N(2)	1.999(7)
Cu(1)	N(2)	1.999(7)
V(1)	V(2)	2.865(2)
V(1)	O(1)	1.611(6)
V(1)	O(2)	1.920(5)
V(1)	O(2)	1.915(5)
V(1)	O(3)	2.020(5)
V(1)	O(6)	1.992(5)
V(2)	O(2)	1.952(5)
V(2)	O(3)	1.968(6)
V(2)	O(4)	1.982(5)
V(2)	O(5)	1.599(5)
V(2)	O(6)	1.945(6)
V(3)	O(3)	1.799(5)
V(3)	O(4)	1.680(5)
V(3)	O(6)	1.818(6)
V(3)	O(7)	1.610(6)

The layers in the compounds have a formal charge of -2 per guest complex. In all cases, local charge neutrality is achieved by direct coordination of apical oxygen atoms to the transition metal guest. These oxide–transition metal interactions are particularly important in **1**, in which only one bidentate ligand per Ni ion was used in the synthesis, and this strategy may be useful in future syntheses directed at layer-bound metal complex fragments. Covalent bonding between the extended oxide host and the guest metal complex should maximize electronic interactions between the two. The availability of mixed-valent vanadium oxide sheets and the variability of oxidation states and photoredox properties of potential guest complexes suggest that a rich variety of magnetically and photochemically interesting oxide–transition metal complex solids may be accessible by similar hydrothermal reactions. Further syntheses along these lines, as well as the characterization of the magnetic and optical properties of this class of compounds, are currently contemplated.

Acknowledgements

P.J.O. and T.E.M. thank the National Science Foundation (CHE-9529202) for support. J.Z.

acknowledges funding from the National Science Foundation (CHE-9617232).

References

[1] H. Kessler, in: G. Alberti, T. Bein (Eds.), Comprehensive Supramolecular Chemistry, Vol. 7, Elsevier, Oxford, UK, 1996, pp. 426-464.
[2] S.L. Burkett, M.E. Davis, in: G. Alberti, T. Bein (Eds.), Comprehensive Supramolecular Chemistry, Vol. 7, Elsevier, Oxford, UK, 1996, pp. 465-483.
[3] R.C. Haushalter, L.A. Mundi, Chem. Mater. 4 (1) (1992) 31.
[4] J.L. Colón, C. Yang, A. Clearfield, C.R. Martin, J. Phys. Chem. 92 (1998) 5777.
[5] J.L. Colón, C. Yang, A. Clearfield, C.R. Martin, J. Phys. Chem. 94 (1990) 874.
[6] B. Shpeizer, D.M. Poojary, K. Ahn, C.E.Runyan Jr., A. Clearfield, Science 266 (1994) 1357.
[7] Y.K. Shin, D.G. Nocera, J. Am. Chem. Soc. 114 (1992) 1264.
[8] D. Papoutsakis, J.E. Jackson, D.G. Nocera, Inorg. Chem. 35 (1996) 800.
[9] J. LeBideau, J.E. Jackson, D.G. Nocera, J. Am. Chem. Soc. 119 (1997) 1313.
[10] Mallouk, T.E., Kim, H.-N., Ollivier, P.J., Keller, S.W., in: G. Alberti, T. Bein (Eds.), Comprehensive Supramolecular Chemistry, Vol. 7, Elsevier, Oxford, UK, 1996, pp. 189-218.
[11] S.W. Keller, S.A. Johnson, E.S. Brigham, E.H. Yonemoto, T.E. Mallouk, J. Am. Chem. Soc. 117 (1995) 12879.
[12] D.M. Kaschak, T.E. Mallouk, J. Am. Chem. Soc. 118 (1996) 4222.
[13] Y. Zhang, J.R.D. DeBord, C.J. O'Connor, R.C. Haushalter, A. Clearfield, J. Zubieta, Angew. Chem. Int. Ed. Engl. 35 (9) (1996) 989.
[14] J.R.D. DeBord, Y. Zhang, R. Haushalter, J. Zubieta, C.J. O'Connor, J. Solid State Chem., 122(2) (1996) 251. D. Hagerman, C. Zubieta, R. Haushalter, J. Zubieta, Angew. Chem. Int. Ed. Engl., 36 (1997) 873.
[15] P.J. Zapf, C.J. Warren, R.C. Haushalter, J. Zubieta, Chem. Commun. 0 (1997) 1543.
[16] teXsan: Texray Structural Analysis Package (revised), Molecular Structure Corporation, The Woodlands, TX, USA, 1995.
[17] G.M. Sheldrick, SHELXS86, in: G.M. Sheldrick, C. Kruger, R. Goddard (Eds.), Crystallographic Computing 3, University Press, 1985, pp. 175.
[18] N. Walker, D. Stuart, Acta Crystallogr., Sect. A 39 (1983) 158.
[19] D. Braga, F. Grepioni, K. Biradha, V.R. Pedireddi, G.R. Desiraju, J. Am. Chem. Soc. 117 (1995) 3156.
[20] G.R. Desiraju, Acc. Chem. Res. 24 (1991) 290.
[21] J.A.R.P. Sarma, G.R. Desiraju, Acc. Chem. Res. 19 (1986) 222.
[22] F.A. Cotton, L.M. Daniels, G.T. Jordan, IV, C.A. Murillo, J. Chem. Soc. Chem. Commun. (1997) 1673.
[23] I.D. Brown, K.K. Wu, Acta Crystallogr., Sect. B 32 (1976) 1957.